Pergamon

Bioorganic & Medicinal Chemistry Letters 10 (2000) 1193–1197

BIOORGANIC & MEDICINAL CHEMISTRY LETTERS

COBRA-1, A Rationally-Designed Epoxy-THF Containing Compound with Potent Tubulin Depolymerizing Activity as a Novel Anticancer Agent

Shyi-Tai Jan, Chen Mao, Alexei O. Vassilev, Christopher S. Navara and Fatih M. Uckun*

Drug Discovery Program and Parker Hughes Cancer Center, Parker Hughes Institute, St. Paul, MN 55113, USA

Received 1 March 2000; accepted 22 March 2000

Abstract—A novel mono-THF containing synthetic anticancer drug, **COBRA-1**, was designed for targeting a previously unrecognized unique narrow binding cavity on the surface of α-tubulin. **COBRA-1** inhibited GTP-induced tubulin polymerization in cell-free tubulin turbidity assays. Treatment of human breast cancer and brain tumor (glioblastoma) cells with **COBRA-1** caused destruction of microtubule organization and apoptosis. Like other microtubule-interfering agents, **COBRA-1** activated the pro-apoptotic c-Jun N-terminal kinase (JNK) signal transduction pathway, as evidenced by rapid induction of *c-jun* expression.

Microtubules are cytoskeletal polymers formed by the parallel association of protofilaments, linear polymers of αβ-tubulin heterodimers. Microtubules play a pivotal role in mitotic spindle assembly and cell division.[1–5] Recently, the structure of the αβ tubulin dimer was resolved by electron crystallography of zinc-induced tubulin sheets.[6] According to the reported atomic model, each 46×40×65 Å tubulin monomer is made up of a 205 amino acid N-terminal GTP/GDP binding domain with a Rossman-fold topology typical for nucleotide-binding proteins, a 180 amino acid intermediate drug-binding domain comprised of a mixed β sheet and five helices that contains the binding sites for both taxol and vinca alkaloids, and a predominantly helical C-terminal domain implicated in the binding of microtubule-associated protein (MAP) and motor proteins.[2,5] The structures of α- and β-tubulin are essentially identical except α-tubulin has a longer S(β-strand)9-S10 loop (in red and pink, Fig. 1) on the inside surface due to an 8 amino acid insertion (Fig. 1, in red), that may stabilize the M-loop (residues 279–287, colored in yellow; see Fig. 1) which plays a very important role for the lateral interaction between parallel protofilaments.[7] The nucleation and organization of microtubules at the γ-tubulin[8] containing microtubule organizing centers plays a critical role for their dynamic instability[9] and cellular function. Microtubules are attached to the microtubule organizing centers via the α-subunits at their minus ends. Because of the continued presence of GTP in α-tubulin and the stabilized M-loop, the last lateral contact between the α-tubulin subunits at the minus end is very strong.[7] Currently available tubulin binding anticancer drugs, including new taxol derivatives and epothilones, interact with β-tubulin and have no effect on microtubule minus ends.[10] Furthermore, cancer cells with an altered β-tubulin expression profile may be resistant to these agents.[11]

In a systematic search for novel drug binding pockets within the intermediate domain of tubulin, we recently discovered a previously unidentified region with a remarkable abundance of leucine and isoleucine residues which could provide a highly hydrophobic binding environment for small molecule organic compounds.[12] Notably, this unique region, which is located near the S9–S10 loop of α-tubulin (or part of the taxol binding site of β-tubulin), contains a narrow cavity with elongated dimensions which could accommodate a fully stretched aliphatic chain with a length of up to 12 carbon atoms (Fig. 1). The enclosure of this putative binding cavity in α-tubulin (but not β-tubulin) is provided in part by the S9–S10 loop (residues 361–368).

A comprehensive structure search of the organic compound files in the Parker Hughes Cancer Center (PHCC)

*Corresponding author. Tel.: +1-612-697-9228; fax: +1-612-697-1042; e-mail: fatih@mercury.ih.org

0960-894X/00/$ - see front matter
PII: S0960-894X(00)00212-2

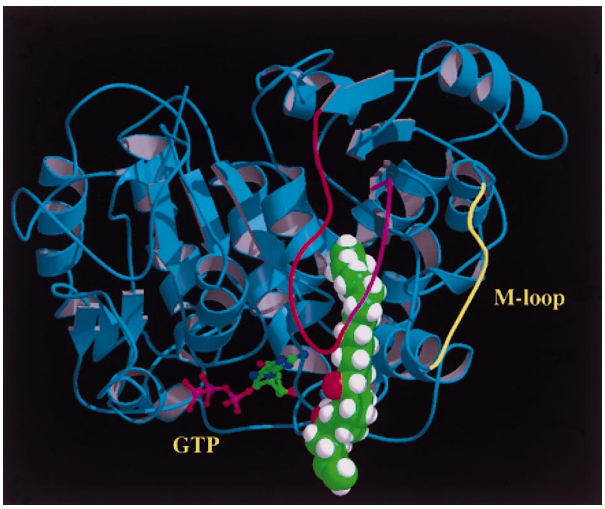

Figure 1. A ribbon representation of the α-tubulin structure (blue) and a space-filling model of the compound **COBRA-1** (green and white) which was docked into the binding site of α-tubulin, based on the electron crystallographic structure of tubulin.[6] Most of the residues in the binding site are identical for α and β tubulin. The binding site on α tubulin has an eight amino acid insertion (residues 361–368, colored in red) which provides additional hydrophobic contact and constitutes the major difference from the taxol binding site on β-tubulin. The compound **COBRA-1** forms extensive interactions with the leucine/isoleucine-rich region near the S9–S10 loop (red and pink) on α-tubulin. The M-loop is colored in yellow and GTP binding site is indicated. The figure was prepared by Molscript and Raster3-D.[17–19]

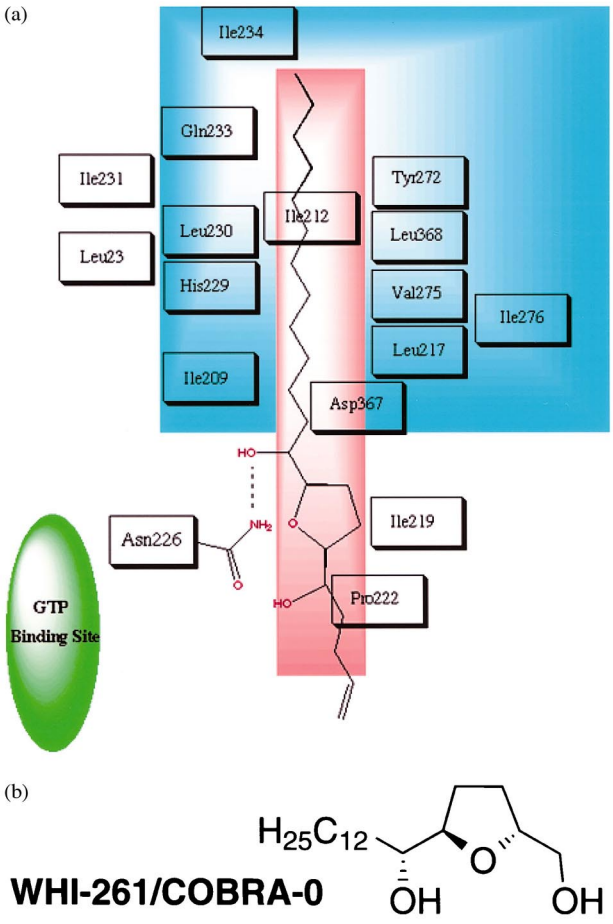

Figure 2. A schematic drawing of **COBRA-1** interacting with protein residues in the target binding pocket of α-tubulin.

Drug Discovery Program led to the identification of a novel mono-THF containing synthetic anticancer drug (**WHI-261**) as the first enantiomerically pure prototype compound targeting this unique binding cavity in α-tubulin.[12] This compound was designated **COBRA-0** because of its mono-THF head portion attached to a long aliphatic chain resembling the shape of a cobra (Fig. 2.). The C_{12} aliphatic side chain of **COBRA-0** is capable of forming hydrophobic interactions with this leucine-rich binding cavity of tubulin. The THF moiety with two flagging hydroxy groups of **COBRA-0** further enhanced the interactions between **COBRA-0** and the novel binding cavity of tubulin by forming hydrogen bonding interactions with the Asn226 residue of tubulin. The THF binding region is more hydrophilic and compatible with the hydroxyl group and oxygen atom of the THF ring. Our modeling studies indicated that the THF binding region is relatively exposed and more forgiving in accommodating different substitutents on the THF ring at the opposite side of the long chain.[12]

In a systematic effort aimed at identifying a simple methodology required for an efficient and flexible synthetic entry into the **COBRA** system that will allow the preparation of related cytotoxic compounds, we explored the addition of a substituent to the primary alcohol carbon of **COBRA-0** as shown in **COBRA-1** (Fig. 2). The new compound **COBRA-1** maintained all of the favorable binding features of **COBRA-0** for the **COBRA** binding pocket of α-tubulin and displayed the same tubulin depolymerizing and apoptosis-inducing properties as **COBRA-0**. **COBRA-1** provides the opportunity for future modifications due to its newly added double bond. Herein, we report the modeling design, synthesis and bioactivity of this novel epoxy-THF containing synthetic compound as a new tubulin depolymerizing anticancer agent. Also provided is unprecedented evidence that **COBRA-1** activates the pro-apoptotic c-Jun N-terminal kinase (JNK) signal transduction pathway, as evidenced by rapid induction of *c-jun* expression.

The enantiomerically pure THF-epoxide **1**, which was synthesized in a straightforward fashion from the commercially available tridecanal **2** in 11 steps with an overall yield of 24%,[13] was reacted with allylmagnesium bromide to form **COBRA-1** (Scheme 1).[14] **COBRA-1** was docked into the putative binding pocket near the taxol binding site of β-tubulin and the same region of α-tubulin using the Affinity module within the INSIGHTII program. This binding pocket has approximate dimensions of 6×22×7 Å (Fig. 1). The long aliphatic chain of **COBRA-1** can interact with the leucine and isoleucine residues 23, 209, 212, 217, 219, 234, 231, 230, 368 and 276 (Fig. 2). Additionally, the THF rings of **COBRA-1** can form favorable interactions with tubulin via hydrogen bonds with residue Asn226 on α tubulin. The results of our molecular modeling and docking studies[15] indicated

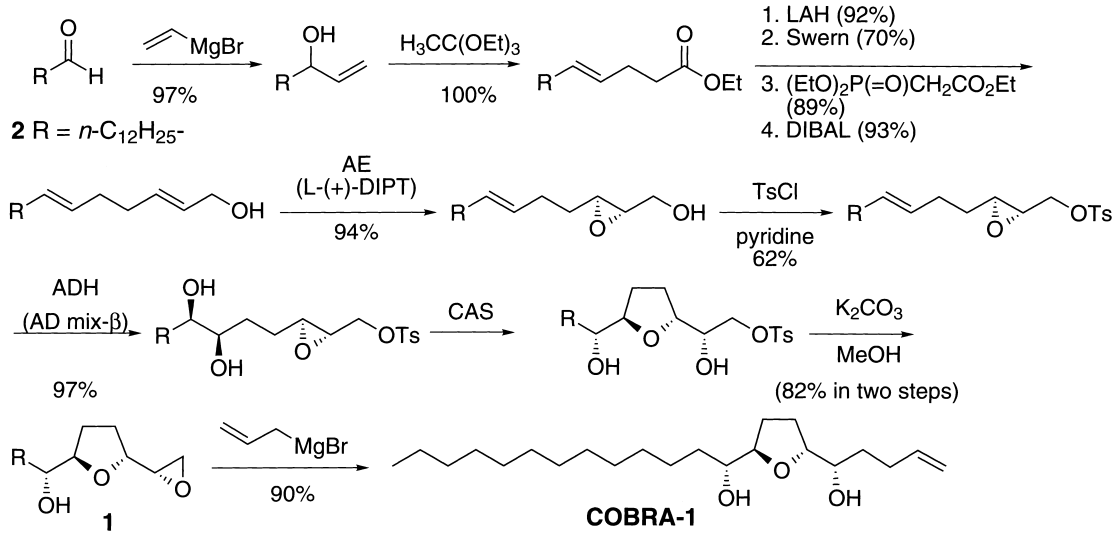

Scheme 1. Synthesis of **COBRA-1**.

that **COBRA-1** would fit much better the binding cavity on α-tubulin than the corresponding region on β-tubulin because of an enclosure on the target binding cavity which is provided in part by the S9–S10 loop in α-tubulin (residues 361–368), which is not present in β-tubulin. **COBRA-1** has a total molecular surface area of 350 Å^2 (defined by Connolly[16]), approximately 256 Å^2 of which is in contact with the binding pocket on α tubulin based on our calculations.

Our molecular modeling studies indicated that **COBRA-1** interacts with the S9–S10 loop on α-tubulin and may therefore destabilize the adjacent M-loop, which is otherwise well positioned for the strong lateral contact with neighbouring subunits. The destabilization of the M-loop on α-tubulin by **COBRA-1** is likely to weaken the concerted interaction between parallel protofilaments at the minus ends of the microtubule and disrupt microtubule dynamics. In accordance with this proposed mode of action, **COBRA-1** inhibited tubulin polymerization in the presence of GTP (Fig. 3), as measured by cell-free tubulin turbidity assays.[20]

The immediate early response gene *c-jun* is induced in response to a diverse set of cytotoxic agents and is directly involved in the molecular signaling of the final common pathway of programmed cell death (i.e., apoptosis). *c-jun* Induction is triggered by activation of the c-Jun N-terminal kinase (JNK), which leads to enhanced *c-jun* transcription by phosphorylation of Jun at sites that increase its ability to activate transcription.[21] Microtubule-interefering agents, including paclitaxel, docetaxel, vinblastine, vincristine, nocodazole, and colchicine have been shown to activate the JNK/*c-jun* signaling pathway in human cancer cells.[22] The activation of the JNK/*c-jun* signaling pathway results in phosphorylation and inactivation of the anti-apoptotic protein BCL-2.[23] To determine if human cancer cells show a similar *c-jun* response to **COBRA-1** treatment, we treated BT-20 breast cancer cells with 25–250 μM **COBRA-1** for 4 h and examined total RNA harvested from cells immediately after treatment for

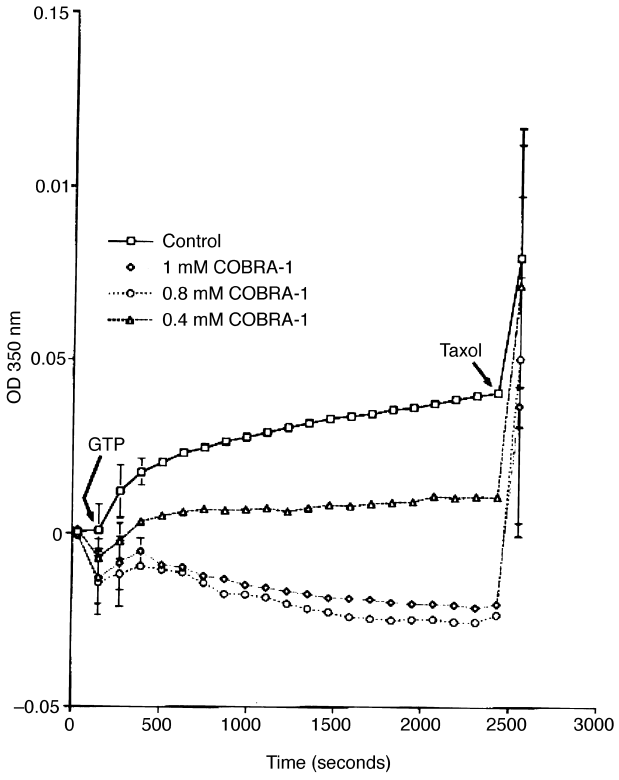

Figure 3. Effect of **COBRA-1** on GTP-Dependent Tubulin Polymerization. Bovine brain tubulin (Sigma, St. Louis, MO) was used in standard turbidity assays to test the effects of **COBRA-1** on GTP-induced tubulin polymerization. **COBRA-1** (in 1% DMSO) was added to tubulin (1 mg/mL, 0.1 M MES, 1 mM EGTA, 0.5 mM $MgCl_2$, 0.1 mM EDTA, 2.5 M glycerol, 1 μg/mL leupeptin, 1 μg/mL aprotinin, pH 6.5) followed by stimulation of polymerization with 1 mM GTP at 2 min and 1 mM taxol at 40 mins. Optical density was measured using a Becton Dickinson UV spectrophotometer (350 nm) using a thermostatted cuvette holder to keep the reaction at 37 °C. Readings obtained from the spectrophotometer were standardized by subtracting the background absorbance of the compound in water from the sample reading following drug addition. **COBRA-1** caused partial depolymerization of tubulin and inhibited its polymerization in the presence of GTP. **COBRA-1** treated tubulin remained responsive to taxol-induced stabilization.

expression levels of *c-jun* mRNA by quantitative Northern blot analysis, as previously described.[24] As shown in Figure 4, **COBRA-1** exposure increased the level of *c-jun* mRNA expression in a concentration-dependent manner without significantly affecting the β-actin control transcript levels, with a maximum stimulation index (as determined by comparison of the c-jun/β-actin ratios in vehicle-treated control cells versus **COBRA-1** treated cells) of 8.5 at 250 μM. Similar results were obtained with U373 glioblastoma cells (data not shown).

Treatment of BT-20 breast cancer and U373 glioblastoma cells with high micromolar concentrations of **COBRA-1** caused destruction of microtubule organization and apoptosis, as documented by confocal laser scanning microscopy (Fig. 5).[25] These effects are reminiscent of the pro-apoptotic effects of other tubulin-binding cytotoxic agents which disrupt microtubule dynamics.[26] At low micromolar concentrations (1–10 μM), **COBRA-1** inhibited the proliferation of BT-20 and U373 cells by impairing the mitotic spindle assembly which is essential for cell division (data not shown).

We next examined the cytotoxic activity of **COBRA-1** against clonogenic NALM-6 leukemia and PC-3 prostate cancer cells using standard in vitro clonogenic assays.[27] Cells were treated with 0.1, 1, 10 and 100 μM of **COBRA-1** for 18 h at 37 °C/5% CO_2, washed, and assayed for clonogenic growth in methylcellulose cultures, as previously described.[27] Clonogenic growth of NALM-6 and PC-3 cells was not affected by **COBRA-1** at concentrations < 10 μM. Notably, **COBRA-1** killed >99% of clonogenic NALM-6 cells and 91% of clonogenic PC-3 cells at 10 μM. **COBRA-1** abrogated the clonogenic growth of both cell lines at 100 μM, which corresponds to >99.9% kill (data not shown).

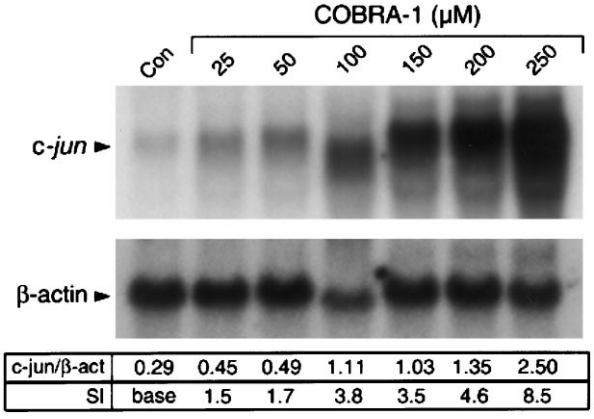

c-jun/β-act	0.29	0.45	0.49	1.11	1.03	1.35	2.50
SI	base	1.5	1.7	3.8	3.5	4.6	8.5

Figure 4. **COBRA-1**-induced activation of the pro-apoptotic *c-jun* signal transduction pathway in human cancer cells. BT-20 human breast cancer cells were treated with the indicated concentrations of **COBRA-1** for 4 h after which total RNA was extracted. Twenty μg of total RNA was denatured in formaldehyde/formamide loading dye (Ambion, Austin, TX) containing 0.2 mg/mL ethidium bromide, at 65 °C for 5 min. RNA was then immediately loaded onto a 1% agarose/formaldehyde gel and electrophoresed at 2 V/cm for 2.5 h. The RNA was transferred to a positively charged nylon membrane by downward capillary transfer in 20× sodium chloride — sodium citrate buffer. Northern blot membranes were hybridized to the *c-jun* probe radiolabeled by random priming with [α^{32}P] dCTP (3000 Ci/mM) (Amersham Pharmacia Biotech) overnight at 42°C in Ambion's hybridization buffer. Unbound probe was removed by washing at 42°C to a final stringency of 1XSSC/0.1%SDS. Results were visualized by autoradiography. The blots were then stripped in boiling 0.1% SDS for 5 min, and rehybridized with the human β-actin probe to normalize for loading differences. The *c-jun* stimulation indices were calculated using the GS-525 Phosphoimager System (Bio-Rad) for quantitative scanning.

In conclusion, we used a three-dimensional computer model of tubulin constructed based upon its recently resolved electron crystallographic structure for rational design of a novel mono-THF containing synthetic anticancer drug targeting a unique narrow binding cavity on the surface of tubulin. Our modeling studies predicted a high affinity interaction of **COBRA-1** with a unique hydrophobic binding site on tubulin located between the GDP/GTP binding site and the M-loop. This unique binding pocket on α-tubulin has elongated dimensions and was predicted to favorably interact with the aliphatic side chain of **COBRA-1**. The modeling studies also indicated that **COBRA-1** is capable of favorable interactions with tubulin via hydrogen bonding with Asn226 residue. Modeling studies of the novel mono-THF containing synthetic anticancer agent **COBRA-1** docked into the target binding site of tubulin revealed additional sterically available space which could be successfully exploited for the design of potentially more effective analogues of this novel anticancer agent. It is noteworthy that curacin A, a thiazoline-containing cytotoxic natural product from the marine cyanobacterium *Lynbya majuscula* that has been reported to interact with the colchicine binding site[28] on tubulin, also contains a long aliphatic chain that shows resemblance to the aliphatic chain in **COBRA-1**. However, curacin A contains a unique header group and a branched, unsaturated C14 chain that differs from the saturated, unbranched C12 chain in **COBRA-1**. These structural differences between curacin A and **COBRA-1** may lead to different binding conformations upon interaction with tubulin. Nevertheless, curacin A is structurally more similar to **COBRA-1** than it is to colchicine. Therefore, this cyanobacterial lipid may exert its cytotoxic activity

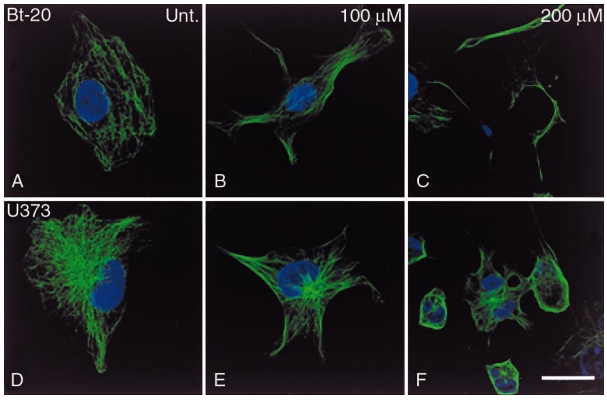

Figure 5. Cytotoxicity of **COBRA-1** against breast cancer and brain tumor cells as documented by Confocal Microscopy. BT-20 breast cancer cells and U373 brain tumor cells are large cells with a well organized microtubule cytoskeleton (A). When treated for 24 h with **COBRA-1** the cells shrink and the microtubules become less organized. Treatment with 100–200 μM **COBRA-1** results in cell death with nuclear fragmentation and complete loss of microtubule formation. Green = microtubules, blue = DNA, Bar = 20 μm.

at least in part by interacting with the **COBRA-1** binding site on tubulin.

References and Notes

1. Avila, J. *Life Sci*. **1992**, *50*, 327.
2. Hyams, J. S.; Lloyd, C. W. *Microtubules*; New York, 1994.
3. Hyman, A.; Karsenti, E. *J Cell Sci*. **1998**, *111*, 2077.
4. Downing, K. H.; Nogales, E. *Curr. Opin. Cell Biol*. **1998**, *10*, 16.
5. Kozielski, F.; Arnal, I.; Wade, R. H. *Curr. Biol*. **1998**, *8*, 191.
6. Nogales, E.; Wolf, S. G.; Downing, K. H. *Nature* **1998**, *391*, 199.
7. Erickson, H. P. *Cell* **1995**, *80*, 367.
8. Oakley, B. R. In *Microtubules*; Hyams, J. S.; Lloyd, C. W., Eds.; Wiley-Liss: New York, 1994, pp 33–45.
9. Desai, A.; Mitchison, T. J. *Ann. Rev. Dev. Biol*. **1997**, *13*, 83.
10. Derry W. B.; Wilson L.; Jordan M. A.; *Cancer Res*. **1998**, *58*, 1177. Jordan A.; Hadfield, J. A.; Lawrence N. J.; McGown, A. T. *Med. Res. Rev*. **1998**, *18*, 259. Shi, Q.; Chen, K.; Morris-Natschke, S. L.; Lee, K. H. *Curr. Pharmaceut. Des*. **1998**, *4*, 219.
11. Ranganathan, S.; Benetatos, C. A.; Colarusso, P. J.; Dexter, D. W.; Hudes, G. R. *Brit. J. Cancer* **1998**. *77*, 562. Derry, W. B.; Wilson, L.; Khan, I. A.; Luduena, R. F.; Jordan, M. A. *Biochemistry* **1997**, *36*, 3554.
12. Uckun, F. M.; Mao, C.; Vassilev, A. O.; Navara, C. S.; Narla, R. K. S.; Jan, S.-T. *Bioorg. Med. Chem. Lett*. **2000**, *10*, 1015.
13. Jan, S. T.; Li, K.; Vig, S.; Rudolph, A.; Uckun, F. M. *Tetrahedron Lett*. **1999**, *40*, 193.
14. Characterization data, of **COBRA-1**: $[\alpha]_d^{22}$ +24.3° (*c* 0.20, $CDCl_3$); ^1H NMR ($CDCl_3$) δ 5.83–5.69 (m, 1H), 5.01–4.89 (m, 2H), 3.83–3.72 (m, 3H), 3.33–3.31 (m, 1H), 2.44 (s, 1H), 2.25–1.76 (m, 6H), 1.65–1.18 (m, 24H), 0.88–0.78, (t, 3H, $J=6.5$ Hz); ^{13}C NMR ($CDCl_3$) δ 138.21, 114.85, 83.39, 82.17, 74.36, 70.87, 33.14, 31.92, 31.63, 30.21, 29.65, 29.35, 28.63, 25.56, 25.34, 22.69, 14.13; IR (neat) 3421, 2922, 2850, 1635, 1067, 669 cm^{-1}; HRMS *m*/*e* (M + 1) calcd 355.3134, found 355.3212.
15. Bohm, H. J. *J. Comput. Aided. Mol. Des*. **1994**, *8*, 243.
16. Connolly, M. L. *Science* **1983**, *221*, 709.
17. Bacon, D. J.; Anderson, W. F. *J. Mol. Graphics* **1988**, *6*, 219.
18. Merritt, E. A.; Murphy, M. E. P. *Acta Cryst*. **1994**, *D50*, 869.
19. Kraulis, P. *J. Appl. Cryst*. **1991**, *24*, 946.
20. Jaing, J. D.; Davis, A. S.; Middleton, K. M.; Bekesi, J. G. *Cancer Res*. **1998**, *58*, 5389.
21. Chae, H. P.; Jarvis, L.; Uckun, F. M. *Cancer Res*. **1993**, 53, 447. Karin, M.; Liu, Z.; Zandi, E. *Curr. Opin. Cell Biol*. **1997**, *9*, 240. Goodman, P. A.; Niehoff, L. B.; Uckun, F. M. *J. Biol. Chem*. **1998**, *273*, 17742.
22. Wang, T. H.; Wang, H. S.; Ichijo, H.; Giannakakou, P.; Foster, J. S.; Fojo, T.; Wimalasena, J. *J. Biol. Chem*. **1998**, *273*, 4928. McCloskey, D. E.; Kaufmann, S. H.; Prestigiacomo, L. J.; Davidson, N. E. *Clin. Cancer Res*. **1996**, *2*, 847. Shtil, A. A.; Mandlekar, S.; Yu, R.; Walter, R. J.; Hagen, K.; Tan, T. H.; Roninson, I. B.; Kong, A. N. *Oncogene* **1999**, *18*, 377. Lee, L. F.; Li, G.; Templeton, D. J.; Ting, J. P. *J. Biol. Chem*. **1998**, *273*, 28253.
23. Srivastava, R. K.; Mi, Q. S.; Hardwick, J. M.; Longo, D. L.; *Proc. Natl. Acad. Sci. USA* **1999**, *96*, 3775. Yamamoto, K.; Ichijo, H.; Korsmeyer, S. J. *Mol. Cell Biol*. **1999**, *19*, 8469.
24. Chae, H. P.; Jarvis, L.; Uckun, F. M. *Cancer Res*. **1993** *53*, 447. Goodman, P. A.; Niehoff, L. B.; Uckun, F. M. *J. Biol. Chem*. **1998**, **273**, 17742.
25. Uckun, F. M.; Waddick, K. G.; Mahajan, S.; Jun, X.; Takata, M.; Bolen, J.; Kurosaki, T. *Science* **1996**, *273*, 1096. Mahajan, S.; Ghosh, S.; Sudbeck, E.; Zheng, Y.; Downs, S.; Hupke, M.; Uckun, F. M. *J. Biol. Chem.,*1999, *274*, 9587. Ghosh, S.; Zheng, Y.; Jun, X.; Narla, R. K.; Mahajan, S.; Navara, C.; Mao, C.; Sudbeck, E. A.; Uckun, F. M. *Clin. Cancer Res*. **1998**, 4, 2657. Vassilev, A.; Ozer, Z.; Navara, C.; Mahajan, S.; Uckun, F. M. *J. Biol. Chem*. **1999**, *274*, 1646. Sudbeck, E.; Liu, X.-P.; Narla, R. K.; Mahajan, S.; Ghosh, S.; Mao, C.; Uckun, F. M. *Clin. Cancer Res*. **1999**, *5*, 1569.
26. Haldar, S.; Chintapalli, J.; Croce, C. M. *Cancer Res*. **1996**, *56*, 1253. Blagosklonny, M. V.; Schulte, T.; Nguyen, P.; Trepel, J.; Neckers, L. M. *Cancer Res*. **1996**, *56*, 1851. Uckun, F. M.; Mao, C.; Vassilev, A. O.; Huang, H.; Jan, S.-T. *Bioorg. Med. Chem. Lett*. **2000**, *10*, 541. Wesselborg, S.; Engels, H.; Rossman, E.; Los, M.; Schultze-Osthoff, K. M. *Blood* **1999**, *93*, 3053. Guise, S.; Braguer, D.; Remacle-Bonnet, M.; Pommier, G.; Briand, C. *Apoptosis* **1999**, *4*, 47.
27. Uckun, F. M.; Evans, W. E.; Forsyth, C. J.; Waddick, K.; G.; T-Ahlgren, L.; Chelstrom, L. M.; Burkhardt, A.; Bolen, J.; Myers, D. E. *Science* **1995**, *267*, 886–891. Uckun, F. M.; Stewart, C. F.; Reaman, G.; Chelstrom, L. M.; Jin, J.; Chandan-Langlie, M.; Waddick, K. G.; White, J.; Evans, W. E. *Blood* **1995** *85*, 2817–2828.
28. Verdier-Pinard, P.; Sitachitta, N.; Rossi, J. V.; Sachkett, D. L.; Gerwich, W. H.; Hamel, E. *Arch. Biochem. Biophys*. **1999**, *1*, 518.